Acquiring multi-spectral images by digital still cameras based on XYZLMS interim connection space

Xiandou Zhang (张显斗)*, Qiang Wang (王 强), Genfu Yang (杨根福), and Mengmeng Wang (王萌萌)

School of Digital Media and Art Design, Hangzhou Dianzi University, Hangzhou 310018, China

**Corresponding author: xiandouzhang@126.com*

Received June 24, 2014; accepted September 11, 2014; posted online October 24, 2014

A method based on the XYZLMS interim connection space is proposed to accurately acquire the multi-spectral images by digital still cameras. The XYZLMS values are firstly predicted from RGB values by polynomial model with local training samples and then spectral reflectance is constructed from XYZLMS values by pseudo-inverse method. An experiment is implemented for multi-spectral image acquisition based on a commercial digital still camera. The results indicate that multi-spectral images can be accurately acquired except the very dark colors.

OCIS codes: 330.1715, 330.1730, 110.4234.
doi: 10.3788/COL201412.113302.

Multi-spectral images have great application prospects in digital arching, computer vision, computer graphics, high-fidelity color representation, and reproduction[1–3]. There are many techniques for multi-spectral image acquisition, such as multi-sensor based, filter based, and light-emitting diode (LED) light sources-based multi-spectral imaging systems[4]. Although they can accurately obtain multi-spectral images, most of these systems are complicated, expensive, and inconvenient, which prevent many practical applications, such as those in common illuminating environments with cameras to get multi-spectral images[5]. Many methods have been proposed to predict the spectral reflectance from RGB values of digital cameras, such as the widely used Wiener method[6,7] and the constrained least-squares (CLS) method[8]. In this work, a method based on common digital still cameras is proposed to acquire multi-spectral images, and an experiment is implemented to verify the performance of the proposed method.

The greatest difficulty for common cameras to acquire multi-spectral images is that there are only three channels in the cameras. It is generally believed that at least six channels are required to accurately acquire multi-spectral images[9]. The XYZLMS interim connection space has been proposed to accurately represent multi-spectral images[10]. If the XYZLMS values can be accurately predicted from RGB values, then multi-spectral images can be accurately acquired from the common cameras. The XYZ values can be accurately predicted from RGB values with polynomial, back propagation (BP) neural network, and look-up table (LUT) methods[11]. Then the key point is that how to predict LMS values from RGB values. Figure 1 shows the $x(\lambda)$, $y(\lambda)$, $z(\lambda)$, $l(\lambda)$, $m(\lambda)$, and $s(\lambda)$ stimulus values in the XYZLMS space, and the spectral sensitivity functions $r(\lambda)$, $g(\lambda)$, and $b(\lambda)$ of a Cannon 60D commercial camera, which is measured by a spectrophotometer[12]. It appears that the L and S values cannot be accurately predicted as the correlation relationship between $l(\lambda)$, $s(\lambda)$ and $r(\lambda)$, $g(\lambda)$, $b(\lambda)$ is low. Fortunately, the spectral reflectances of real-world objects are smooth functions of wavelength[13]. The L and S values somehow have the same variation trend with the RGB values, which can connect the correlation relationship between RGB and L, S values. In other words, there are great possibilities for the prediction of L and S values from RGB values for real-world objects. To verify this point, an experiment was implemented for the Z value prediction from RGB values, and similar conclusion can be derived for the L and S values prediction. As shown in Fig. 1, there is little correlation relationship between $z(\lambda)$ and $r(\lambda)$, so both of the following polynomial models were adopted for the Z value prediction to investigate whether the R values have contribution to the Z value prediction.

$$Z = a_0 + a_1 r + a_2 g + a_3 b + a_4 r^2 + a_5 g^2 + a_6 b^2 + a_7 rg + a_8 rb + a_9 gb + a_{10} rgb, \quad (1)$$

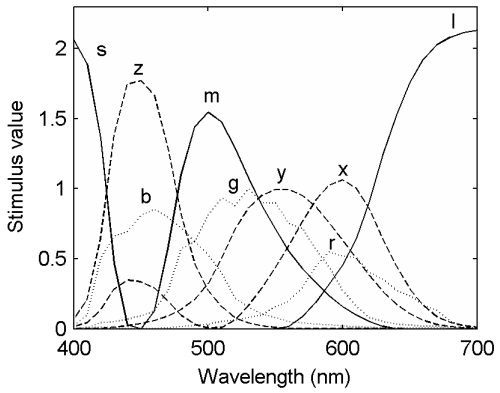

Fig. 1. Spectral distribution of the nine stimulus values.

$$Z = c_0 + c_1 g + c_2 b + c_3 g^2 + c_4 b^2 + c_5 gb, \tag{2}$$

where r, g, and b denote the RGB values normalized by the maximum RGB values of the captured image, and $a_s (s = 0, 1 \cdots 10)$ and $c_t (t = 0, 1 \cdots 5)$ denote the coefficients of the polynomial model.

The Z value of each color patch in Gretag Macbeth ColorChecker Semi Gloss (CCSG) color chart was predicted with the other color patches as training samples. The mean and maximum errors of predicted Z values for all the color patches are 0.55 and 2.32 for Eq. (1), while for Eq. (2) are 0.77 and 3.13, respectively, which indicated that R values play an important role in the Z value prediction, although there is no strong correlation relationship between $z(\lambda)$ and $r(\lambda)$.

For each object with spectral reflectance $r(\lambda)$, the corresponding XYZLMS values can be calculated by

$$\begin{cases} X = k_1 \int_{\lambda_{\min}}^{\lambda_{\max}} I_1(\lambda) x(\lambda) r(\lambda) \, \mathrm{d}\lambda, \\ Y = k_1 \int_{\lambda_{\min}}^{\lambda_{\max}} I_1(\lambda) y(\lambda) r(\lambda) \, \mathrm{d}\lambda, \\ Z = k_1 \int_{\lambda_{\min}}^{\lambda_{\max}} I_1(\lambda) z(\lambda) r(\lambda) \, \mathrm{d}\lambda, \end{cases} \tag{3}$$

$$\begin{cases} L = k_2 \int_{\lambda_{\min}}^{\lambda_{\max}} I_2(\lambda) l(\lambda) r(\lambda) \, \mathrm{d}\lambda, \\ M = k_2 \int_{\lambda_{\min}}^{\lambda_{\max}} I_2(\lambda) m(\lambda) r(\lambda) \, \mathrm{d}\lambda, \\ S = k_2 \int_{\lambda_{\min}}^{\lambda_{\max}} I_2(\lambda) s(\lambda) r(\lambda) \, \mathrm{d}\lambda, \end{cases} \tag{4}$$

$$k_1 = \frac{100}{\int_{\lambda_{\min}}^{\lambda_{\max}} I_1(\lambda) y(\lambda) \, \mathrm{d}\lambda}, \tag{5}$$

$$k_2 = \frac{100}{\int_{\lambda_{\min}}^{\lambda_{\max}} I_2(\lambda) m(\lambda) \, \mathrm{d}\lambda}, \tag{6}$$

where $I_1(\lambda)$ and $I_2(\lambda)$ denote the spectral power distributions of the illuminants, and $\lambda_{\min}$ and $\lambda_{\max}$ represent the minimum and maximum values of the spectral wavelength in the visible light range. The variables in Eqs. (3)–(6) can be sampled on the range from 400 to 700 nm at 10 nm intervals without significant loss of accuracy for most applications. Then the XYZLMS values can be determined by

$$\mathbf{t} = \mathbf{F}\mathbf{r}, \tag{7}$$

where $\mathbf{t}$ is a 6×1 matrix and represents the XYZLMS values, $\mathbf{F}$ is a 6×31 matrix with rows being the samples of $I_1(\lambda)x(\lambda)$, $I_1(\lambda)y(\lambda)$, $I_1(\lambda)z(\lambda)$, $I_2(\lambda)l(\lambda)$, $I_2(\lambda)m(\lambda)$, and $I_2(\lambda)s(\lambda)$, respectively, and $\mathbf{r}$ is a 31×1 matrix and represents the spectral reflectance of a sample.

There are two steps for the multi-spectral images acquisition, XYZLMS values prediction from RGB values and spectral reflectance construction from XYZLMS values. Various methods can be used for XYZLMS prediction and spectral reflectance construction. The 11 terms polynomial model[14] is adopted for the XYZLMS value prediction in this work. The forms of the polynomial model for XYZLMS value prediction are similar as Eq. (1). The polynomial model with n training samples could be written as

$$\mathbf{A} = \mathbf{M}\mathbf{C}, \tag{8}$$

where $\mathbf{A}$ is a n×6 matrix and represents the XYZLMS values of the n training samples, $\mathbf{M}$ is a n×11 matrix and denotes the terms of the polynomial model, and $\mathbf{C}$ is a 11×6 matrix and denotes the coefficients of the polynomial model. As the corresponding relationship between RGB and XYZLMS values varies with the RGB location in the RGB color gamut, it is difficult to accurately estimate all the XYZLMS values with only one transformation matrix. So the local training samples were adaptively selected for each candidate sample according to the RGB location in the color gamut. Then the coefficient matrix $\mathbf{C}$ can be determined by the least-squares method with the selected local training samples as

$$\mathbf{C} = (\mathbf{M}'\mathbf{M})^{-1}\mathbf{M}'\mathbf{A}, \tag{9}$$

where the prime mark and superscript "–1" means matrix transpose and inverse, respectively.

After the XYZLMS values are predicted with the polynomial model, the pseudo-inverse method[15] is employed for the spectral reflectance construction from the predicted XYZLMS values in this work. The spectral reflectance $\tilde{\mathbf{r}}$ can be constructed based on Eq. (7) as

$$\tilde{\mathbf{r}} = \mathbf{W}\mathbf{t}_1, \tag{10}$$

where $\mathbf{t}_1$ is a 6×1 matrix and represents the predicted XYZLMS values. $\mathbf{W}$ is the 31×6 matrix that denotes the transformation matrix, which is determined by

$$\mathbf{W} = \mathbf{N}_t \times \mathbf{PINV}(\mathbf{T}_t), \tag{11}$$

where $\mathbf{N}_t$ is a 31×l matrix, $\mathbf{T}_t$ is a 6×l matrix, $\mathbf{N}_t$ and $\mathbf{T}_t$ represent the spectral reflectance and XYZLMS value sets of the selected local training samples, respectively, and $\mathbf{PINV}(\mathbf{T}_t)$ means the Moore–Penrose pseudo-inverse of matrix $\mathbf{T}_t$.

To verify the spectral image acquisition accuracy of the proposed XYZLMS method, the CCSG and two printed color charts, LUT, and European Color Initiative (ECI) color chart were used as training and testing samples. The LUT color chart, with notes of 0, 20, 40, 60, 80, and 100 for each of the C, M, Y, and K channel, totally contained 1296 color patches, covering the whole color gamut of the printer. The ECI color chart, with 1485 color patches evenly distributed in the CMYK color space, has been widely used in the colorimetric characterization of printer and press. The LUT and ECI color charts were printed by an HP Desk Jet ink printer, and the corresponding spectral reflectance of each patch in

the two color charts was measured by an X-rite i1isis automatic scanning spectrophotometer after the color charts were totally naturally dried out. The raw images of CCSG and two printed color charts were captured by a Cannon 60D commercial camera under the Huali CPL-124Z fluorescent light source. The focal length of the camera was set to 58 mm, aperture size was $f/5.6$, shutter speed was 1/6 s, ISO was 100, resolution was 5184×3456, and bit depth was 14. The mean RGB value in the central 30×30 pixel region was calculated to represent the RGB response of each color patch in the color charts.

The raw RGB values of the LUT, ECI, and CCSG color charts were firstly normalized by the maximum RGB values of the captured image. Here the maximum RGB value is 4000. Then the normalized RGB values and corresponding measured spectral reflectance of the LUT color chart were adopted as training samples for parameter determination of the polynomial and pseudo-inverse models. The normalized RGB values of the ECI and CCSG color charts combining with the corresponding measured spectral reflectance were used to verify the spectral reflectance construction accuracy of the proposed method. The colorimetric prediction accuracy of the ECI and CCSG color charts are listed in Table 1, in which the CIEDE2000 color differences[16–18] of the measured and estimated spectral reflectance were calculated under CIE illuminants (A, D50, D65, D90, F2, F7, F11) and four actual LED light sources (LED1: Cooper DL11, LED2: GE Par30, LED3: OsramDiachroic, LED4: SoluxDiachroic)[19], respectively.

The results of Table 1 show that the colorimetric prediction accuracies are extremely high for the ECI color chart, whereas a little lower for the CCSG color chart. The main reason is that there is still somewhat media metamerism problem[20,21] for the spectral image acquisition based on digital cameras when the media of training and testing samples are different. In fact, the estimated spectral reflectance of the CCSG color charts with bigger errors are mainly concentrated in the dark colors (Fig. 2), which illustrates the measured and estimated spectral reflectances of the patches with CIEDE2000 color differences[22] greater than 4. This is because that the signal-to-noise ratio of RGB value is low for the dark colors. In other words, the RGB errors are relatively high for the dark colors, which firstly affected the prediction accuracy of the XYZLMS values, then further affected the spectral reflectance construction accuracy. In addition, the correlations between the RGB and XYZLMS values are low as the RGB and XYZLMS values are small for the dark colors, which also increased the prediction errors in XYZLMS values, further affecting the spectral reflectance construction accuracy. This phenomenon also happens to other multispectral imaging systems. Table 1 also shows that there are no significant differences for the prediction accuracy under different illuminants and light sources both for the ECI and CCSG color charts, which indicates that the prediction accuracies have no wavelength selectivity although there are only three color channels in the camera and some wavelength in the visible light range was little covered by the three spectral sensitivity functions. In addition, the mean CIEDE2000 color differences under all the illuminants and light sources are 1.05 and 2.11 for ECI and CCSG color charts, respectively, and they are both within the color difference tolerance in the printing industry[22], which indicates that the proposed method has great practical application prospect.

To further verify the spectral prediction accuracy and compare the proposed XYZLMS method with other methods, the Wiener[6] and CLS methods[8] were also

Table 1. Colorimetric Prediction Accuracy of the Proposed XYZLMS Method

		ECI			CCSG		
		Mean	**Max.**	**%>4**	**Mean**	**Max.**	**%>4[a]**
ΔE^*_{00}	A	1.066	4.699	0.202	2.503	9.351	18.750
	D50	1.044	4.347	0.269	1.649	9.940	4.167
	D65	1.037	4.233	0.202	2.000	10.033	7.292
	D90	1.035	4.227	0.135	2.563	10.107	20.833
	F2	1.069	4.351	0.067	2.118	9.181	5.208
	F7	1.040	4.195	0.202	1.960	10.200	5.208
	F11	1.048	4.400	0.269	1.744	10.330	4.167
	LED1	1.064	4.282	0.067	2.210	9.329	12.500
	LED2	1.092	4.598	0.202	2.478	9.310	17.708
	LED3	1.064	4.778	0.202	2.345	9.485	16.667
	LED4	1.045	4.439	0.269	1.653	9.872	4.167

[a]%>4 represents the percentage of testing samples with color differences greater than 4 CIEDE2000 units.

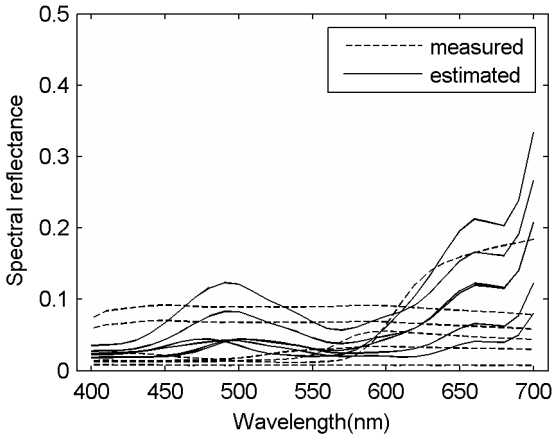

Fig. 2. Measured and estimated spectral reflectances of the CCSG color chart with color differences greater than 4.

Table 2. Spectral Prediction Accuracy of the XYZLMS, Wiener, and CLS Methods

	RMSE			**GFC**		
	Min.	**Mean**	**Max.**	**Min.**	**Mean**	**Max.**
XYZLMS	0.0005	0.0102	0.0416	0.9960	0.9998	1.0000
Wiener	0.0023	0.0156	0.0470	0.9886	0.9992	1.0000
CLS	0.0025	0.0184	0.0541	0.9394	0.9988	1.0000

implemented with the LUT and ECI color chart as training and testing samples, respectively. The statistical results of root-mean-square error (RMSE) and goodness-of-fit coefficient (GFC)[23] between the measured and predicted spectral reflectance is shown in Table 2. The results indicate that the proposed XYZLMS method performed better than the Wiener and CLS methods both according to the RMSE and GFC criteria. In addition, the proposed method is much more efficient than the other methods as the XYZLMS values can be directly used in spectral image compression and gamut mapping in spectral image reproduction[10].

In conclusion, the colorimetric and spectral prediction accuracies of the proposed method are high for the ECI and CCSG color charts except the dark colors, and the prediction accuracies have no wavelength selectivity. The proposed method can be used to acquire multi-spectral images, especially when the media of training samples are designed same as the candidate object requiring spectral image acquisition. Another advantage of the proposed method is that the predicted XYZLMS values can be directly used for spectral image reproduction as the XYZLMS space is a competitive interim connection space in the spectral color management system.

This work was supported by the National Natural Science Foundation of China (No. 61205168) and the National Science and Technology Support Program of China (No. 2012BAH91F03).

References

1. M. S. Drew and A. Y. Salekdeh, Dig. Photo **VII,** 23 (2011).
2. J. D. Tian and Y. D. Tang, Opt. Lett. **38,** 2818 (2013).
3. Y. Li, D. Lu, and L. Zhao, Chin. Opt. Lett. **11,** 113301 (2013).
4. W. P. Yang, N. Xu, J. J. Duan, Y. B. Li, Q. Lu, Y. Sun, X. Luo, and Y. D. Luo, J. Yunnan Univ. National. **18,** 191 (2009).
5. J. Jiang and J. W. Gu, in *Proceedings of IEEE Workshop on the Computer Vision and Pattern Recognition* 1 (2012).
6. P. Stigell, K. Miyata, and M. H. Kasari, Pattern Recogn. Image Anal. **17,** 233 (2007).
7. H. L. Shen and J. H. Xin, J. Opt. Soc. Am. A **21,** 1125 (2004).
8. C. J. Li and M. R. Luo, in *Porceedings of IS&T/SID 13th Color Imaging Conference* 99 (2005).
9. J. Redman, in *International Conference on Digital Printing Technologies and Digital Fabrication* 355 (2007).
10. X. D. Zhang, Q. Wang, Y. Wang, and H. Z. Wu, Opt. Lett. **37,** 5097 (2012).
11. G. Sharma, *Digital Color Imaging Handbook* (CRC Press, 2003).
12. J. Jiang, D. Y. Liu, J. W. Gu, and S. Susstrunk, in *Proceedings of IEEE Workshop on the Applications of Computer Vision* (2013).
13. D. Y. Tzeng and R. S. Berns, Color. Res. Appl. **30,** 84 (2005).
14. G. W. Hong, M. R. Luo, and P. A. Rhodes, Color. Res. Appl. **26,** 76 (2001).
15. N. Shimano, K. Terai, and M. Hironaga, J. Opt. Soc. Am A **24,** 3211 (2007).
16. M. R. Luo, G. Cui, and B. Rigg, Color. Res. Appl. **26,** 340 (2001).
17. Z. Wang and H. Xu, Chin. Opt. Lett. **12,** 023301 (2014).
18. Q. Tong, H. Xu, and R. Gong, Chin. Opt. Lett. **11**, 073301 (2013).
19. "Spectral power distribution (SPD) curves," http://research.ng-london.org.uk/scientific/spd/
20. Z. J. Li and R. S. Berns, Color. Res. Appl. **32,** 293 (2007).
21. X. D. Zhang and H. S. Xu, J. Opt. Soc. Am A **25,** 371 (2008).
22. H. X. Liu, B. Wu, Y. Liu, M. Huang, and Y. F. Xu, Appl. Mech. Mater. **262,** 96 (2013).
23. J. Ruiz, "Quality metrics for spectral estimation," Master Thesis (Universitat Politècnica de Catalunya, 2010).